IEEE Access
Multidisciplinary | Rapid Review | Open Access Journal

Received December 2, 2017, accepted February 14, 2018, date of publication February 28, 2018, date of current version March 16, 2018.

Digital Object Identifier 10.1109/ACCESS.2018.2810318

Mobility Management in Ultra-Dense Networks: Handover Skipping Techniques

ELENI DEMARCHOU, (Student Member, IEEE), CONSTANTINOS PSOMAS, (Member, IEEE), AND IOANNIS KRIKIDIS, (Senior Member, IEEE)

KIOS Research and Innovation Center of Excellence, Department of Electrical and Computer Engineering, University of Cyprus, Nicosia 1678, Cyprus

Corresponding author: Eleni Demarchou (edemar01@ucy.ac.cy)

This work was supported in part by the Research Promotion Foundation, Cyprus, through the Project COM-MED under Grant KOINA/ERANETMED/1114/03, in part by the European Union's Horizon 2020 Research and Innovation Program under Grant 739551 (KIOS CoE), and in part by the Government of the Republic of Cyprus through the Directorate General for European Programs, Coordination, and Development.

ABSTRACT Ultra-dense network deployment is a key technology for potentially achieving the capacity target of next-generation wireless communication systems. However, such a deployment results in cell proliferation and cell size decrement, leading to an increased number of handovers and limited sojourn time within a cell, which severely degrade the user's quality of service (QoS). In this paper, we propose two intelligent handover skipping techniques to overcome the high handover rates. The first technique considers a user associated with a single base station (BS) and the decision to skip a handover is based on the upcoming cell's topology; we consider three criteria: 1) the area of the cell; 2) the trajectory distance within the cell; and 3) the distance of the BS from the cell edge. The second technique exploits BS cooperation and enables a dynamic handover skipping scheme, where the skipping decision is taken based on the BSs of three consecutive cells in the user's trajectory. This technique achieves a balance between BS cooperation and single BS transmission and manages to maintain a good QoS during the skipping phase. We show that the proposed techniques reduce both the handover rate and handover cost and outperform the conventional techniques for moderate to high-velocity values.

INDEX TERMS Handover, ultra-dense networks, base station cooperation, stochastic geometry, second-order Voronoi.

I. INTRODUCTION

In recent years, mobile devices and cellular subscriptions have become more prevalent causing an ever-increasing data traffic and subsequently straining out the available resources [2]. In order to meet the forthcoming requirements, researchers have set the target of 1000-fold increment to the current fourth generation's (4G) capacity [3]. Specifically, the future fifth generation (5G) wireless communications systems are expected to provide service to a tremendous amount of users offering higher data rates and lower end-to-end latencies, while supporting high-mobility users. It has been shown that, a significant increase to the users' quality of service (QoS) can be achieved by the deployment of denser networks. This is a consequence of the smaller cells which are deployed, achieving better area spectral efficiency as frequency reuse becomes more efficient [5]. To that end, ultra-dense network deployment has been proposed as a key technology to make the capacity target attainable [4]. However, even though the benefits for stationary users in ultra-dense networks are unambiguous, the support of mobile users requires special management in order to maintain a decent QoS along their trajectory.

Conventionally, mobile users change connectivity every time they enter a different cellular cell; this process is referred to as handover. Despite the fact that this ensures a user is within service along its trajectory, each handover execution costs in system resources [6]. This is due to the delay in connection switching, which subsequently affects the user's QoS [7]. Compared to conventional networks, ultra-dense networks are composed of a larger number of small cells. Therefore, in such networks, handover executions occur more frequently since a user crosses more cells along it's trajectory and moves inside each cell for a limited time. In this case, the handover cost increases significantly and becomes crucial for a mobile users' performance in terms of the average throughput. The users are thus required to allocate

most of their resources for the handover executions instead for data traffic, which substantially degrades their QoS [8]. Consequently, mobility management in ultra-dense networks requires the design of more intelligent handover techniques to overcome these limitations.

Regarding mobility management, various studies exist in the literature. Hong *et al.* [9] study the handover process between a macro and a small cell in heterogeneous networks and provide closed-form expressions for the sojourn time within a small cell by using tools from stochastic geometry. Merwaday *et al.* [10] consider spatial randomness and exploit the user's trajectory path to provide a velocity estimation algorithm. Bao and Liang [11] consider base station (BS) cooperation to study a user-centric cooperative network and provide theoretical results for the handover and average downlink rates. A joint BS assignment and bandwidth allocation scheme is proposed in [12], by taking into account users with different mobility and traffic profiles. Arshad *et al.* [13] introduce an alternating handover skipping scheme in order to reduce the handover rate. In this scheme, a user executes a handover alternately along its trajectory while associated with either its closest or second closest BS; it is shown that this scheme achieves a 50% reduction of the handover rate. This work is extended in [14] and [15], where the authors exploit BS cooperation to improve the user's performance when a handover is skipped. In addition, they introduce the concept of topology-based handover skipping, where a handover is skipped based on the user's distance from the target BS and the size of the cell.

In this work, we study mobility management for ultra-dense networks and propose two intelligent handover skipping techniques to reduce a user's handover rate. We take into account various topological characteristics of the network, which are used by our proposed techniques to decide whether or not to skip a handover. Specifically, the contribution of our work is two-fold:

- We study a handover skipping technique based on the upcoming cell's topology. We consider that the user associates with it's closest BS and the handover decision is taken based on one of the following criteria: (a) the area of the cell, (b) the trajectory distance within the cell, and (c) the distance of the BS from the cell edge. Specifically, if the value of the criterion is less than a pre-defined threshold, then the handover is skipped. In contrast to [15], a rigorous mathematical analysis is provided. Our results show that for low and high velocities, the proposed technique converges to the conventional and alternating skipping, respectively, whereas for moderate velocities our proposed technique outperforms both.
- We propose an intelligent handover skipping technique by exploiting the topological properties which result from BS cooperation. In contrast to our first proposed technique and the one in [14], we manage to diminish the randomness of the user's associated BSs during the skipping phase. Specifically, a handover is skipped when the next two consecutive cells along a user's trajectory have a BS in common with the current associated BSs. As such, while in [14] and [15], BS cooperation is used as a performance booster during the skipping phase, in this work, the user always enjoys the cooperative gain, unless a handover is skipped. In this way, we can reduce the handover rate and achieve a balance between cooperative transmissions and single BS transmission.

The rest of the paper is organized as follows. Section II presents the system model and Section III describes the proposed handover skipping schemes. Section IV provides the analysis for the average throughput and Section V presents the numerical results. Finally, Section VI concludes our work.

Notation: $\mathbb{R}^2$ is the two-dimensional Euclidean space; $\|x\|$ is the Euclidean norm of x; $\mathbb{P}(X)$ represents the probability of the event X with expected value $\mathbb{E}(X)$; ${}_2F_1(\cdot,\cdot;\cdot;\cdot)$ denotes the Gauss hypergeometric function and $\Gamma(\cdot)$ is the complete Gamma function [16].

II. SYSTEM MODEL

Consider a downlink cellular network where the BSs are randomly distributed in the two dimensional Euclidean plane $\mathbb{R}^2$, according to a homogeneous Poisson point process (PPP) $\Phi = \{x_k \in \mathbb{R}^2\}$, $k \geq 1$, with density λ; x_k denotes the coordinates of the k-th BS. Each BS is equipped with a single antenna and transmits with power P. We consider a centralized architecture (e.g. cloud radio access network), which enables the employment of BSs cooperation, and assume the user associates with its K closest BSs in the network. As a result, the Euclidean plane $\mathbb{R}^2$ is sectored by a Poisson Voronoi tessellation of order K. Specifically, a Voronoi cell $\mathcal{V}_{\mathcal{S}}^{(K)}$ formed by the set $\mathcal{S} = \{x_1, \ldots, x_K\} \subset \Phi$, is defined as the region consisting of the points closer to the ones in $\mathcal{S}$ than any other points in Φ i.e.,

$$\mathcal{V}_{\mathcal{S}}^{(K)} = \{z \in \mathbb{R}^2 \mid \forall\, x \in \mathcal{S}, y \in \Phi \setminus \mathcal{S}, \|x - z\| \leq \|y - z\|\}. \tag{1}$$

All wireless signals in the network are assumed to experience small-scale Rayleigh fading. Therefore, the channel gain h_k from the k-th BS to the user is exponentially distributed and unit variance is assumed i.e., $h_k \sim \exp(1)$. In addition, we take into account the large-scale path-loss effect which follows the power-law function $r_k^{-\alpha}$, where $r_k = \|x_k\|$, $x_k \in \Phi$, is the distance from the k-th BS to the origin and $\alpha > 2$ is the path-loss propagation exponent. We assume the BSs are sorted in ascending order with respect to their distance from the origin i.e., $r_k \leq r_{k+1}, \forall x_k \in \Phi$. Then, the probability density function (PDF) of the distance r_k to the k-th closest BS, is given by [17]

$$f(r_k) = \frac{2(\pi\lambda)^k}{\Gamma(k)} r_k^{2k-1} \exp(-\pi\lambda r_k^2), \tag{2}$$

and the joint PDF of the distances to the k closest BSs is [17]

$$f(r_1, \ldots, r_k) = (2\lambda\pi)^k \exp(-\lambda\pi r_k^2) r_1 \cdots r_k. \tag{3}$$

Let $\mathcal{N} = \{x_1, \ldots, x_k\} \subset \Phi$, $k \geq 1$, denote the locations of the BSs which are instantaneously associated with the user. The associated BSs are considered to employ non-coherent joint transmission (NCJT), which is a low complexity scheme with no channel state information requirements and thus it is suitable for high mobility users [15]. In addition, an ideal successive interference cancellation (SIC) scheme is assumed, where the user can draw out the strongest interfering signals. Therefore, the instantaneous signal-to-interference-plus-noise ratio (SINR) at the user is

$$\text{SINR} = \frac{\left|\sum_{x_k \in \mathcal{N}} \sqrt{P h_k r_k^{-\alpha}}\right|^2}{I_n + \sigma^2}, \tag{4}$$

where σ^2 is the power of the additive white Gaussian noise and $I_n = P\sum_{x_i \in \Phi} h_i r_i^{-\alpha}$, $i > n$ refers to the aggregate interference occurring from the n-th closest BS and onwards, where n defines the number of BSs associated with the user together with the ones that have been cancelled using SIC.

Assume a mobile user crossing the network with an arbitrary trajectory and velocity v. Along this trajectory, the user's connections change according to its location such that the user maintains its connectivity with the network. Conventionally, the user is always associated with its K closest BSs i.e., a handover is triggered when the user crosses the boundaries of a K-th order Voronoi cell. In this case, the handover rate is given by [11]

$$H_c^{(K)} = \frac{\Gamma(0.5+K)}{\pi^{3/2}\Gamma(K)} 8v\sqrt{\lambda}. \tag{5}$$

In the following, we consider two scenarios with $K = 1$ and $K = 2$, and exploit the topological characteristics of the Voronoi tessellation provided by each case. For these scenarios, we present our proposed handover techniques according to which the user can dynamically skip an upcoming handover process.

III. HANDOVER SKIPPING TECHNIQUES

In this section, we assume that a user's mobility pattern can be predicted based on its trajectory and velocity [13], [18] and present two intelligent handover skipping techniques: a non-cooperative (NC) and a cooperative (CO) technique.

A. NON-COOPERATIVE SKIPPING TECHNIQUE (NC)

Consider a user traversing the network, associated with its closest BS. Hence, the user along its trajectory crosses the boundaries of first order Voronoi cells i.e., $K = 1$. Assume this trajectory is along the cells $\mathcal{V}_{\mathcal{A}}^{(1)}$ to $\mathcal{V}_{\mathcal{F}}^{(1)}$, as shown in Fig. 1. Conventionally, a handover would occur every time the user would cross the boundaries of each cell. Instead, we propose a handover skipping technique, according to which the user can skip an upcoming handover based on a certain topological criterion X of each cell. Specifically, say the user is located within the cell $\mathcal{V}_{\mathcal{A}}^{(1)}$ moving towards the cell $\mathcal{V}_{\mathcal{B}}^{(1)}$. The decision whether to handoff i.e., drop its connection to the BS of $\mathcal{V}_{\mathcal{A}}^{(1)}$ and connect to the BS of $\mathcal{V}_{\mathcal{B}}^{(1)}$, is taken based on the value X of the cell $\mathcal{V}_{\mathcal{B}}^{(1)}$, denoted by $X_{\mathcal{B}}$, as follows:

- If $X_{\mathcal{B}}$ is less than a pre-defined threshold θ_X, then the handover is skipped. In this case, the user enters the cell $\mathcal{V}_{B}^{(1)}$, maintaining its connection with the BS of cell $\mathcal{V}_{\mathcal{A}}^{(1)}$.
- Otherwise, the handover is executed when the user enters the cell $\mathcal{V}_{B}^{(1)}$. That is, the user drops its current connection and the serving BS becomes the one within the cell $\mathcal{V}_{B}^{(1)}$.

Note that, consecutive handover skipping is avoided in order to maintain the QoS of the user at a decent level. Therefore, the skipping mechanism is under consideration only if the user executed a handover at the previous boundary cross along its trajectory. In what follows, we present the three proposed criteria.

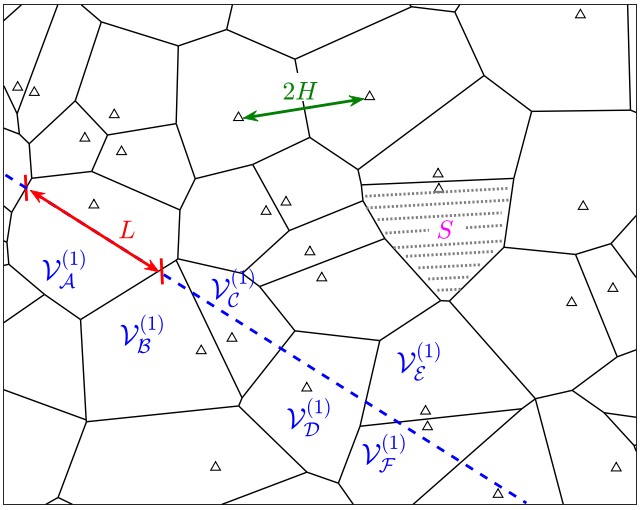

FIGURE 1. First order Poisson Voronoi tessellation with the three criteria; dashed line represents a user's trajectory.

1) AREA OF THE CELL

The first criterion refers to the cell area, denoted by S. When the area of a cell is small, the user's sojourn time within that cell is limited. As a result, the time between two consecutive handovers is minimal. In this case, the user's resources dedicated for data transmission are diminished and subsequently the user's throughput is decreased. Therefore, the handover executions when entering cells with small areas can be avoided.

2) CHORD LENGTH OF THE CELL

The chord, denoted by L, refers to the distance intended to be covered by the user in the upcoming cell. Similarly to the cell area, it aims to avoid frequent handovers due to the limited sojourn time. However, this criterion can be more accurate, as it captures the cases where the area is large but the user's distance within the cell is small. For instance, take the user's trajectories in $\mathcal{V}_{\mathcal{B}}^{(1)}$ and $V_{\mathcal{E}}^{(1)}$, illustrated in Fig. 1. Even though both have relatively large areas, the handovers can be skipped

due to the small trajectory lengths covered by the user within the cells.

3) DISTANCE FROM THE CELL EDGE

The final criterion is the perpendicular distance, denoted by H, between the BS in the upcoming cell and the boundary which will be crossed by the user. This distance determines how close the two BSs of the current and upcoming cell are to each other. Therefore, when this is small, connecting to either BS will provide similar path-loss effects. See for example, cells $\mathcal{V}_{\mathcal{B}}^{(1)}$-$\mathcal{V}_{\mathcal{C}}^{(1)}$ and $\mathcal{V}_{\mathcal{E}}^{(1)}$-$\mathcal{V}_{\mathcal{F}}^{(1)}$ in Fig. 1. Thus, the handover process can be skipped without affecting significantly the user's QoS.

B. COOPERATIVE SKIPPING TECHNIQUE (CO)

We now consider the cooperative case, where the user associates with its closest and second closest BSs in the network. In this case, a second order Poisson Voronoi tessellation is formed, i.e., $K = 2$, and a handover is executed every time the user crosses the boundaries of a second order Voronoi cell. The handover skipping technique described in Section III-A, could also be applied in this scenario. However, we propose a different approach where we exploit the topological properties of the second order Voronoi tessellation. Specifically, the proposed intelligent handover skipping technique ensures that when a handover is skipped, the user remains associated with either its closest or second closest BS, thus maintaining a descent QoS. This is feasible due to the property of second order Voronoi tessellations according to which neighbouring cells have one BS in common. In Fig. 2 for instance, the cells $\mathcal{V}_{\{x_a,x_c\}}^{(2)}$ and $\mathcal{V}_{\{x_c,x_e\}}^{(2)}$ formed by the BSs $\{x_a, x_c\}$ and $\{x_c, x_e\}$, respectively, have x_c as a common BS. A detailed description of the proposed technique is given below.

Consider a mobile user crossing the cells $\mathcal{V}_{\mathcal{A}}^{(2)}$, $\mathcal{V}_{\mathcal{B}}^{(2)}$, and $\mathcal{V}_{\mathcal{C}}^{(2)}$ sequentially, where each of the sets $\mathcal{A}$, $\mathcal{B}$, and $\mathcal{C}$ contains two BSs. Initially, the user is served by the two BSs of the set $\mathcal{A}$. The handover decision when passing from $\mathcal{V}_{\mathcal{A}}^{(2)}$ to $\mathcal{V}_{\mathcal{B}}^{(2)}$ is made based on the BSs that form the cell $\mathcal{V}_{\mathcal{C}}^{(2)}$. Let x_α denote the common BS of the sets $\mathcal{A}$ and $\mathcal{B}$ i.e., $x_\alpha \in \mathcal{A} \cap \mathcal{B}$; and let $x_\beta \in \mathcal{B} \cap \mathcal{C}$. Then,

- if the common BS between the sets $\mathcal{A}$ and $\mathcal{B}$, and the one between $\mathcal{B}$ and $\mathcal{C}$, is the same i.e., $x_\alpha = x_\beta$, then the user enters $\mathcal{V}_{\mathcal{B}}^{(2)}$ skipping the handover process. In this case, the user remains connected with the common BS of the three cells, while dropping its association from the second BS of the set $\mathcal{A}$ i.e., a single BS ensures connectivity.
- If $x_\alpha \neq x_\beta$, then a handover is executed when the user enters $\mathcal{V}_{\mathcal{B}}^{(2)}$. In this case, the serving set becomes $\mathcal{B}$ i.e., two BSs ensure connectivity.

The procedure is iterative and a decision is made at each cell by considering the user's path along three consecutive cells. For example, for the movement along the cells $\mathcal{V}_{\mathcal{B}}^{(2)}$ and $\mathcal{V}_{\mathcal{C}}^{(2)}$, the decision will be made in $\mathcal{V}_{\mathcal{B}}^{(2)}$ according to the path along $\mathcal{V}_{\mathcal{B}}^{(2)}$, $\mathcal{V}_{\mathcal{C}}^{(2)}$, and say $\mathcal{V}_{\mathcal{D}}^{(2)}$. Note that, the steps of the proposed technique and the patterns described above, are not affected when the user is initially connected to a single BS.

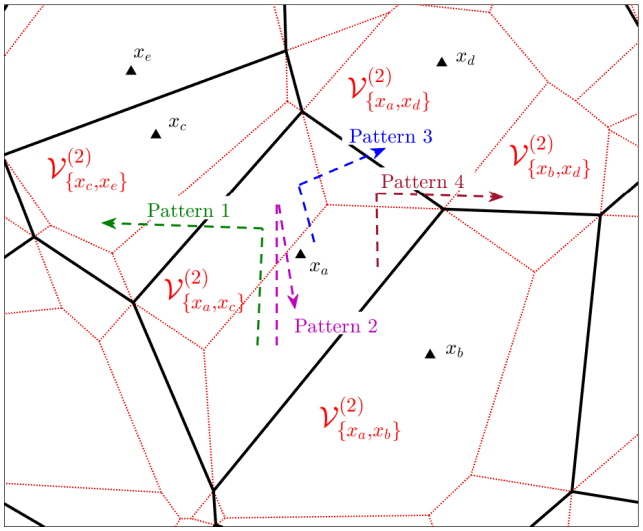

FIGURE 2. First and second order Poisson Voronoi tessellations, depicted with solid and dotted lines, respectively.

IV. HANDOVER SKIPPING PERFORMANCE

In this section, we study the performance of our proposed handover skipping techniques.

A. HANDOVER RATE

The handover rate achieved by each of the proposed techniques is obtained as follows.

1) NC SKIPPING TECHNIQUE

Let $f_X(x)$ denote the PDF of the random variable $X \in \{S, L, H\}$. According to the NC technique, a handover is skipped with probability $\Pi_X(\theta_X) = \mathbb{P}(X < \theta_X)$, which denotes the cumulative distribution function (CDF) of X; both the PDF and CDF of X are given in Appendix A. As already stated, in order to maintain a decent QoS, consecutive cell skipping is avoided. This implies that the proposed technique allows for a maximum reduction of the handover rate by half, achieved when $\Pi_X(\theta_X) = 1$, which corresponds to the alternating skipping [13]. Therefore, along a user's path, the handover rate is reduced by half $\Pi_X(\theta_X) \times 100\%$ of the time. Otherwise, the handover process follows the conventional approach. Thus, the handover rate of a user employing the NC handover skipping technique is given by

$$H_s^{(1)} = \frac{H_c^{(1)}}{2}\Pi_X(\theta_X) + H_c^{(1)}(1 - \Pi_X(\theta_X)), \tag{6}$$

where $H_c^{(1)} = \frac{4}{\pi} v\sqrt{\lambda}$ is given in (5).

2) CO SKIPPING TECHNIQUE

For this case, we need to consider the mobility patterns of a user along three consecutive cells. Without loss of generality, all possible handover decisions can be described in four patterns, illustrated in Fig. 2. According to Patterns 1 and 4,

the common BS x_a of the first two cells is not part of the BSs of the third cell. As such, a handover is executed and the user's serving BSs become $\{x_a, x_c\}$ and $\{x_a, x_d\}$, respectively. On the other hand, for Patterns 2 and 3, the BS x_a is common to all three cells. Thus, when the user enters the second cell, the association with BS x_b is dropped and the user remains solely associated to the common BS x_a. As such, a handover is skipped or executed with equal probability i.e., handover skipping is performed over half the cells along a user's trajectory. Note that, this does not imply that the user will alternately skip a handover, but on average, half of the handovers are skipped. Therefore, the handover rate of a user employing the CO handover skipping technique is expressed as

$$H_s^{(2)} = \frac{H_c^{(2)}}{2} = \frac{3}{\pi} v\sqrt{\lambda}, \tag{7}$$

where $H_c^{(2)} = \frac{6}{\pi} v\sqrt{\lambda}$ is given in (5). It is worth mentioning that (7) is lower than the achieved handover rates of both conventional solutions for $K = 1$ and $K = 2$, that is, $H_s^{(2)} < H_c^{(1)} < H_c^{(2)}$.

Next, we derive the coverage probability and average spectral efficiency of a user.

B. COVERAGE PROBABILITY

The coverage probability $\mathcal{P}$ determines the probability that a user's SINR is above a pre-defined threshold T i.e., $\mathbb{P}(\text{SINR} > T)$. We first derive a general expression and using that, we deduce specific expressions for a user employing the NC and CO techniques. Thus, the coverage probability of a user served with NCJT by the set of BSs $\mathcal{N} = \{x_1, \ldots, x_k\}$, $k \geq 1$, is

$$\begin{aligned}\mathcal{P} &= \mathbb{P}\left(\frac{\left|\sum_{x_i\in\mathcal{N}} \sqrt{P h_i r_i^{-\alpha}}\right|^2}{I_k + \sigma^2} > T\right) \\ &= \mathbb{P}\left(\left|\sum_{x_i\in\mathcal{N}} \sqrt{h_i r_i^{-\alpha}}\right|^2 > \frac{T}{P}(I_k + \sigma^2)\right).\end{aligned} \tag{8}$$

As $h_i \sim \exp(1)$, $\left|\sum_{x_i\in\mathcal{N}} \sqrt{h_i r_i^{-\alpha}}\right|^2$ is an exponential random variable with mean $1/\sum_{x_i\in\mathcal{N}} r_i^{-\alpha}$. By using the complementary CDF of an exponential random variable, we have

$$\begin{aligned}\mathcal{P} &= \mathbb{E}_\Phi\left[\exp\left(-\frac{T}{P}\frac{I_k + \sigma^2}{\sum_{x_i\in\mathcal{N}} r_i^{-\alpha}}\right)\right] \\ &= \mathbb{E}_\Phi\left[\mathcal{L}_{I_k}(s)\exp\left(-\frac{\sigma^2}{P}s\right)\right],\end{aligned} \tag{9}$$

where

$$\mathcal{L}_{I_k}(s) \triangleq \mathbb{E}_{\Phi,h_j}\left[\exp\left(-s\sum_{x_j\in\Phi\setminus\mathcal{N}} h_j r_j^{-\alpha}\right)\right], \tag{10}$$

is the Laplace transform of the interference term I_k and we define $s \triangleq \frac{T}{\sum_{x_i\in\mathcal{N}} r_i^{-\alpha}}$. The Laplace transform is given in the following lemma.

Lemma 1: The Laplace transform $\mathcal{L}_{I_k}(s)$ of the interference term I_k, evaluated at s is given by

$$\mathcal{L}_{I_k}(s) = \exp\left(-\frac{2\pi\lambda s r_k^{2-\alpha}}{\alpha - 2} {}_2F_1\left(1, 1 - \frac{2}{\alpha}; 2 - \frac{2}{\alpha}; -\frac{s}{r_k^\alpha}\right)\right), \tag{11}$$

where $\alpha > 2$ and r_k denotes the distance between the k-th closest BS and the user.

Proof: See Appendix B. □

According to the NC skipping technique, a user is associated with its closest BS. If a handover is skipped, the user remains connected with its previous serving BS even though it enters a new cell. In this case, the closest BS is the one in the new cell while the serving BS is the user's n-th closest BS, where $n \geq 2$. As already mentioned, the user employs an ideal SIC, so when the user is served by the n-th closest BS, $n \geq 2$, the $(n-1)$ strongest interfering signals can be cancelled out. Therefore, using the PDF $f(r_n)$ given by (2), the coverage probability when the user is served by its n-th closest BS i.e., $\mathcal{N} = \{x_n\}$, is

$$\mathcal{P}_{\text{NC}}^{(n)} = \frac{2(\pi\lambda)^n}{\Gamma(n)} \int_0^\infty \mathcal{L}_{I_n}(s) r_n^{2n-1} \exp\left(-\pi\lambda r_n^2 - \frac{\sigma^2}{P}s\right) dr_n, \tag{12}$$

where $\mathcal{L}_{I_n}(s)$ is given by Lemma 1 and $s \triangleq T r_n^\alpha$.

In the CO skipping technique, the user is associated with both its closest and second closest BSs. Then, the serving set is $\mathcal{N} = \{x_1, x_2\}$. In this case, we have $s \triangleq \frac{T}{r_1^{-\alpha} + r_2^{-\alpha}}$ and using the joint PDF $f(r_1, r_2)$ of r_1 and r_2 given by (3), the coverage probability is

$$\begin{aligned}\mathcal{P}_{\text{CO}} = (2\lambda\pi)^2 \int_0^\infty r_1 \int_{r_1}^\infty r_2 \mathcal{L}_{I_2}(s) \\ \times \exp\left(-\lambda\pi r_2^2 - \frac{\sigma^2}{P}s\right) dr_2 dr_1,\end{aligned} \tag{13}$$

where $\mathcal{L}_{I_2}(s)$ is the Laplace transform of the interference occurring from the second closest BS and onwards and is given by Lemma 1. Now, if a handover is skipped, the serving BS is either the user's closest or second closest. Similar to the NC technique, when the user is served by its second closest BS, the interference occurring from the user's closest BS is cancelled out. In this case, the coverage probability is given by (12) with $n = 1$ (closest BS association) or $n = 2$ (second closest BS association).

To simplify the derived expressions, we consider a special case with $\alpha = 4$ and an interference limited scenario i.e., $\sigma^2 = 0$. For this case, the Laplace transform in Lemma 1 can be simplified to [13]

$$\mathcal{L}_{I_n}(s) = \exp\left(-\lambda\pi\sqrt{s}\arctan\left(\frac{\sqrt{s}}{r_n^2}\right)\right), \tag{14}$$

and the coverage probability when the user is connected with its n-th closest BS is given by

$$\mathcal{P}_{\mathrm{NC}} = \left(1 + \sqrt{T}\arctan\left(\sqrt{T}\right)\right)^{-n}. \tag{15}$$

Finally, the coverage probability in the BS cooperation case can be simplified to

$$\mathcal{P}_{\mathrm{CO}} = (2\lambda\pi)^2 \int_0^\infty r_1 \int_{r_1}^\infty r_2 \exp\left(-\lambda\pi r_2^2\right) \times \exp\left(-\lambda\pi\sqrt{\frac{T}{r_2^{-4}+r_1^{-4}}}\arctan\left(\sqrt{\frac{Tr_1^4}{r_1^4+r_2^4}}\right)\right) dr_2 dr_1. \tag{16}$$

From the simplified expression in (15), we can clearly see that as n increases i.e., the user is served by a BS furthest away, the coverage probability decreases. Furthermore, for a fixed n, (15) depends entirely on the threshold T, which is also valid for (16); even though it is not clear from the non-closed form expression, we have numerically validated this remark.

C. SPECTRAL EFFICIENCY

We now evaluate the average spectral efficiency $\mathcal{R}$ achieved by our proposed techniques. This is written as

$$\mathcal{R} = \int_0^\infty \mathbb{P}\left(\log_2(1+\mathrm{SINR}) > x\right) dx. \tag{17}$$

By the change of variable $T \to 2^x - 1$, we have

$$\mathcal{R} = \frac{1}{\ln(2)} \int_0^\infty \frac{\mathbb{P}\left(\mathrm{SINR} > T\right)}{T+1} dT, \tag{18}$$

where $\mathbb{P}(\mathrm{SINR} > T)$ is the coverage probability derived in Section IV-B. When the user employs the conventional techniques, the achieved spectral efficiency is given by

$$\mathcal{R}_c^{(K)} = \frac{1}{\ln(2)} \int_0^\infty \frac{\mathcal{P}_{\mathrm{CN}}^{(K)}}{T+1} dT, \tag{19}$$

where $\mathcal{P}_{\mathrm{CN}}^{(K)}$ is the user's coverage probability when $\mathcal{N} = \{x_1, \ldots, x_K\}$, derived similarly to (13) using (3) over K distances. Note that, $\mathcal{P}_{\mathrm{CN}}^{(1)}$ and $\mathcal{P}_{\mathrm{NC}}^{(1)}$ are equal. Similarly, when the user is served by the n-th closest BS, $n > 1$, the achieved spectral efficiency is

$$\mathcal{R}_n = \frac{1}{\ln(2)} \int_0^\infty \frac{\mathcal{P}_{\mathrm{NC}}^{(n)}}{T+1} dT. \tag{20}$$

To derive the spectral efficiency for each of the proposed handover skipping techniques, we take into account both cases where a handover is skipped or not. Therefore, the achieved spectral efficiency for the proposed handover techniques are given in the following propositions.

Proposition 1: The average spectral efficiency of a mobile user employing the NC skipping technique is given by

$$\mathcal{R}_{\mathrm{NC}} = \frac{1}{2\ln(2)}\left(\Pi_X(\theta_X)\int_0^\infty \frac{\mathcal{P}_{\mathrm{NC}}^{(n)}}{T+1} dT + (2-\Pi_X(\theta_X))\int_0^\infty \frac{\mathcal{P}_{\mathrm{NC}}^{(1)}}{T+1} dT\right), \tag{21}$$

where $\Pi_X(\theta_X)$, $X \in \{S, L, H\}$, is given in Appendix A, $\mathcal{P}_{\mathrm{NC}}^{(1)}$ and $\mathcal{P}_{\mathrm{NC}}^{(n)}$ are given by (12) *and* $n > 1$.

Proof: Based on the NC skipping technique, the user is at least half of the time associated with its closest BS, since consecutive cell skipping is avoided. During the rest of the user's trajectory, a handover is skipped with probability $\Pi_X(\theta_X)$, $X \in \{S, L, H\}$. In this case, the user remains connected with the BS of the previous cell which is no longer its closest BS i.e., $n > 1$. Therefore, we have

$$\mathcal{R}_{\mathrm{NC}} = \frac{1}{2}\mathcal{R}_c^{(1)} + \frac{1}{2}\left(\Pi_X(\theta_X)\mathcal{R}_n + (1-\Pi_X(\theta_X))\,\mathcal{R}_c^{(1)}\right). \tag{22}$$

By replacing $\mathcal{R}_c^{(1)}$ and $\mathcal{R}_n$ with (19) and (20), respectively, the result follows. □

Note that when $\Pi_X(\theta_X) = 1$, the NC technique converges to alternating skipping where half of the time the user is associated with its closest BS and the other half of the time the user is associated with the n-th closest BS, $n > 1$.

Proposition 2: The average spectral efficiency of a mobile user employing the CO skipping technique is given by

$$\mathcal{R}_{\mathrm{CO}} = \frac{1}{4\ln(2)}\left(\int_0^\infty \frac{\mathcal{P}_{\mathrm{NC}}^{(1)}}{T+1} dT + \int_0^\infty \frac{\mathcal{P}_{\mathrm{NC}}^{(2)}}{T+1} dT + 2\int_0^\infty \frac{\mathcal{P}_{\mathrm{CO}}}{T+1} dT\right), \tag{23}$$

where $\mathcal{P}_{\mathrm{NC}}^{(1)}$ and $\mathcal{P}_{\mathrm{NC}}^{(2)}$ are given by (12) *and $\mathcal{P}_{\mathrm{CO}}$ is given by* (13).

Proof: Following the steps of the CO skipping technique, the user associates with its two closest BSs or with only one BS with equal probability. Due to the spatial symmetry, when the user is connected with a single BS, it is either the user's closest or second closest with the same likelihood. Therefore, the average spectral efficiency is the sum of these three scenarios with their corresponding probabilities, that is,

$$\mathcal{R}_{\mathrm{CO}} = \frac{1}{2}\mathcal{R}_c^{(2)} + \frac{1}{2}\left(\frac{1}{2}\mathcal{R}_c^{(1)} + \frac{1}{2}\mathcal{R}_2\right). \tag{24}$$

By replacing $\mathcal{R}_c^{(2)}$ and $\mathcal{R}_2$ with (19) and (20), respectively, the result follows. □

D. AVERAGE THROUGHPUT

Finally, we provide our main performance metric, which is the average throughput of a user employing the proposed handover techniques. The average throughput (bits/s (bps)), denoted by $\mathcal{T}$, is given by [13]

$$\mathcal{T} = B(1-z)(1-d)\mathcal{R}, \tag{25}$$

where B is the available channel bandwidth, z is a constant variable corresponding to the fraction of the resources used for signaling between the user and the BSs and d is the handover cost i.e., the time fraction occupied by the handover execution (no data is transmitted), and is defined as [15]

$$d = \min(\tau H, 1), \tag{26}$$

where τ is the handover delay, H is the handover rate given by (5), (6) and (7) for the conventional, the NC and the CO technique, respectively. Note that when $\tau H > 1$, the sojourn time of the user within a cell is less than the handover delay and therefore the achieved throughput results in 0 bps [15]. Finally, $\mathcal{R}$ is the achieved spectral efficiency (bits/s/Hz) given by (19), (21) and (23) for the conventional, the NC and the CO technique, respectively.

1) COMPARISON WITH CONVENTIONAL TECHNIQUES

The conventional handover techniques achieve a higher spectral efficiency compared to the corresponding proposed skipping techniques i.e., $\mathcal{R}_c^{(1)} > \mathcal{R}_{\text{NC}}$ and $\mathcal{R}_c^{(2)} > \mathcal{R}_{\text{CO}}$. This is due to the fact that, conventionally the user is always connected with its closest BS ($K = 1$) or both its closest and second closest BSs ($K = 2$). On the other hand, the handover cost is reduced when our proposed techniques are employed; note that this cost increases with the user's velocity. Therefore, even though the conventional schemes provide higher average throughput for small values of v, at some value v^*, the handover cost becomes crucial and our proposed techniques outperform the conventional ones. We define v^* as the switching velocity and is evaluated by equating the average throughput of each of the proposed skipping techniques with the corresponding conventional technique and solving with respect to v. For the $K = 1$ scenario, the switching velocity is given by

$$v^* = \frac{\pi\left(\mathcal{R}_n - \mathcal{R}_c^{(1)}\right)}{2\tau\sqrt{\lambda}\left(\mathcal{R}_c^{(1)}\left(\Pi_X(\theta_X) - 4\right) - \mathcal{R}_n\left(\Pi_X(\theta_X) - 2\right)\right)}, \tag{27}$$

where $\mathcal{R}_c^{(1)}$ and $\mathcal{R}_n$ are given by (19) and (20), respectively. Similarly, we provide the switching velocity for the $K = 2$ scenario, given by

$$v^* = \frac{\pi\left(\mathcal{R}_c^{(2)} - \mathcal{R}_s^{(2)}\right)}{3\tau\sqrt{\lambda}\left(2\mathcal{R}_c^{(2)} - \mathcal{R}_s^{(2)}\right)}, \tag{28}$$

where $\mathcal{R}_c^{(2)}$ and $\mathcal{R}_s^{(2)}$ are given by (19) and (23), respectively.

2) COMPARISON WITH ALTERNATING SKIPPING ($K = 1$)

When $\Pi_X(\theta_X) = 1$, the NC technique corresponds to the alternating skipping technique and can achieve a maximum reduction of the handover rate by 50%. However, with alternating skipping the achieved spectral efficiency is the lowest compared to both the conventional and the NC technique with $\Pi_X(\theta_X) < 1$. However, the alternating skipping technique provides lower average throughput than the NC technique up to a certain velocity u^*, after which the handover rate reduction is more critical than the higher spectral efficiency. By following a similar methodology as before we get

$$u^* = \frac{\pi\left(1 - \Pi_X(\theta_X)\right)\left(\mathcal{R}_c^{(1)} - \mathcal{R}_n\right)}{2\tau\sqrt{\lambda}\left(\mathcal{R}_c^{(1)}\left(3 + \Pi_X(\theta_X)\left(\Pi_X(\theta_X) - 4\right)\right) - \mathcal{R}_n\left(1 - \Pi_X(\theta_X)\right)^2\right)}, \tag{29}$$

where $\mathcal{R}_c^{(1)}$ and $\mathcal{R}_n$ are given by (19) and (20), respectively.

Furthermore, it has been shown that the CO technique achieves a lower handover rate than both the conventional solutions for $K = 1$ and $K = 2$. However, alternating skipping for $K = 1$ is the technique which achieves the lowest handover rate such that

$$\frac{H_c^{(1)}}{2} < H_s^{(2)} < H_c^{(1)} < H_c^{(2)}. \tag{30}$$

As a result, even though the spectral efficiency achieved by the CO technique is higher, alternating skipping offers the highest throughput than the CO technique, for velocities higher than

$$u^* = \frac{\pi\left(2\mathcal{R}_c^{(2)} - \mathcal{R}_c^{(1)} - \mathcal{R}_n^{(1)}\right)}{\tau\sqrt{\lambda}\left(6\mathcal{R}_c^{(2)} - \mathcal{R}_c^{(1)} - \mathcal{R}_n^{(1)}\right)}, \tag{31}$$

where $\mathcal{R}_c^{(K)}$ and $\mathcal{R}_n$ are given by (19) and (20), respectively.

V. NUMERICAL RESULTS

Simulation results were carried out to evaluate the proposed handover skipping techniques. We consider the interference-limited scenario ($\sigma^2 = 0$) with $\alpha = 4$. In addition, the channel bandwidth is $B = 10$ MHz, the part of resources dedicated for signaling is set to $z = 0.3$ and the handover delay is $\tau = 0.8$ s [13]. The BS density is set to $\lambda = 10^{-4}$ and the transmit power of each BS is set to $P = 10$ kW. Furthermore, we will refer to the conventional techniques by Conv. $\mathcal{V}^{(1)}$ and Conv. $\mathcal{V}^{(2)}$ for $K = 1$ and $K = 2$, respectively.

Fig. 3 presents the coverage probability versus the threshold SINR T, for BS association scenarios: $\mathcal{N} = \{x_1, x_2\}$ (BS cooperation), $\mathcal{N} = \{x_1\}$ (closest), $\mathcal{N} = \{x_2\}$ (second closest), $\mathcal{N} = \{x_3\}$ (third closest) and $\mathcal{N} = \{x_4\}$ (fourth closest). As expected, when the user is connected with the two closest BSs, the coverage probability is the highest among all the cases. In addition, for the cases where the user associates with a single BS i.e., $\mathcal{N} = \{x_n\}$, $n \geq 1$, we can see that as n increases, the coverage probability decreases. This is due to the increment in the path-loss effects which degrades the received SINR and subsequently the coverage probability.

A. NC SKIPPING TECHNIQUE

We now present the results for the throughput achieved by the NC skipping technique. The considered threshold is $\theta_X = k\mathbb{E}[X]$, $k \in \mathbb{R}^+$, where $\mathbb{E}[X]$ is the expected value of the random variable X. Therefore, the threshold for each criterion is $\theta_S = k/\lambda$, $\theta_L = k\pi/4\sqrt{\lambda}$, and $\theta_H = k(4/\sqrt{\lambda} + \lambda\pi)/3\pi$, evaluated using the PDFs in Appendix A.

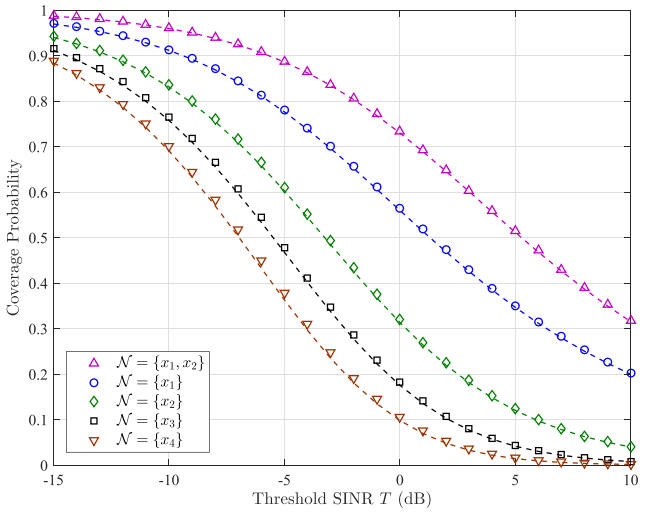

FIGURE 3. Coverage probability versus threshold SINR, dashed lines represent analytical results.

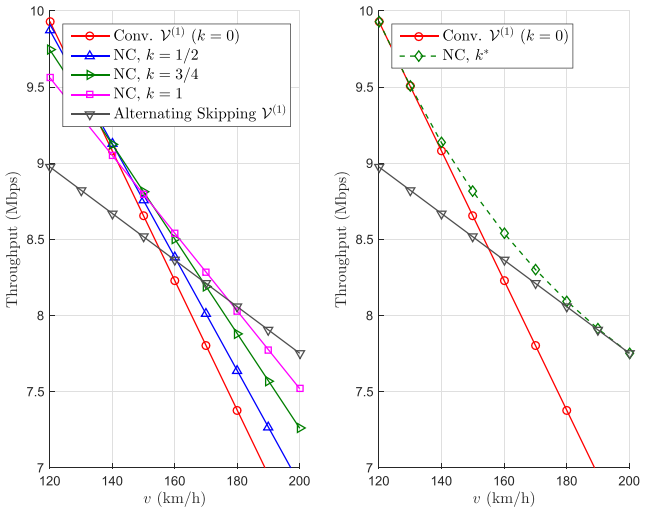

FIGURE 4. Average throughput versus the user's velocity v for $K = 1$; Left: $X = S$, Right: $X \in \{S, L, H\}$.

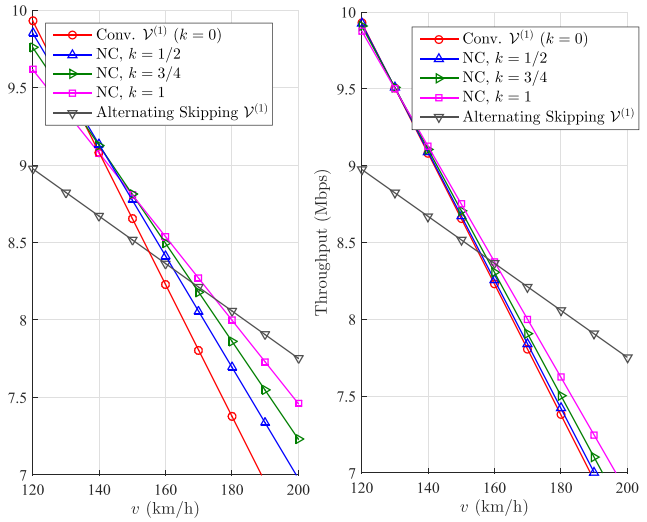

FIGURE 5. Average throughput versus the user's velocity v for $K = 1$; Left: $X = L$, Right: $X = H$.

TABLE 1. Switching velocity v^* (NC vs Conv. $\mathcal{V}^{(1)}$).

	X	$k = 1/2$	$k = 3/4$	$k = 1$
v^* (km/h)	S	131.049	136.246	141.726
	L	132.074	135.75	140.221
	H	127.728	128.896	130.781
	Alternating skipping $(\Pi_X(\theta_X) = 1)$: 155.06			

We consider different values of k, where $k = 0$ corresponds to the conventional handover technique Conv. $\mathcal{V}^{(1)}$. Finally, we assume that during the handover skipping phase, the BS in the previous cell is the user's second closest in the network i.e., x_2.

Fig. 4 presents the average throughput versus the user's velocity v; the left sub-figure considers the case where the handover criterion is the area of the cell i.e, $X = S$. It can be seen that, as the user's velocity increases, the average throughput decreases. This is expected since higher velocities are subject to higher handover rates and handover cost which have a major impact on the average throughput. It is clear that Conv. $\mathcal{V}^{(1)}$ performs better for low values of v whereas our proposed technique outperforms the conventional one for high values of v; the two techniques provide the same performance at the switching velocity v^* which corresponds to their intersection point in the figure. The switching velocity is evaluated analytically in Table 1. Next, we compare our technique with the alternating skipping technique. Our technique outperforms the alternating skipping technique for low velocities whereas for high velocities, our technique does not perform as well. Note that as k increases our technique converges to the alternating skipping technique. The switching velocity u^* corresponds to the intersection point between the NC technique with the alternating skipping and is analytically presented in Table 2.

As such, the NC technique provides a better performance for velocities $v^* < v < u^*$. For example, as illustrated in the first sub-figure, for $k = 1$, our technique achieves the highest average throughput for velocities $142 < v < 175$ km/h. On the other hand, for $v < 142$ and $v > 175$ km/h, the Conv. $\mathcal{V}^{(1)}$ and alternating skipping techniques, respectively, outperform our technique. This is also clear in the second sub-figure, where we present the optimal k, denoted by k^*, that maximizes the average throughput. As can be seen, for moderate velocities i.e., $130 < v < 190$ km/h, the NC technique offers the highest average throughput while for low and high velocities, the NC technique converges to the Conv. $\mathcal{V}^{(1)}$ and alternating skipping techniques, respectively. Note that the results in the second sub-figure, hold for any $X \in \{S, L, H\}$. In Fig. 5, we present the average throughput versus the user's velocity for the other two criteria, L and H, depicted in the first and second sub-figure, respectively. Similar observations can be deduced as before for the effect of k on the performance.

TABLE 2. Switching velocity u^* (alternating skipping vs NC).

	X	$k=1/2$	$k=3/4$	$k=1$
u^* (km/h)	S	160.875	168.778	177.269
	L	162.422	168.018	174.92
	H	155.899	157.642	160.472

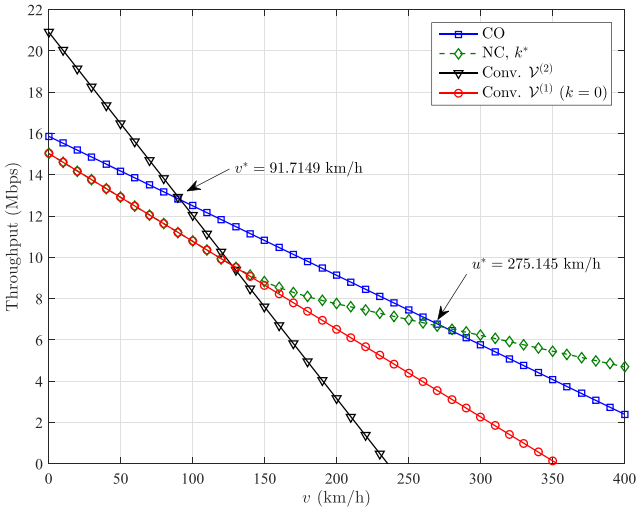

FIGURE 6. Average throughput versus the user's velocity v.

B. CO SKIPPING TECHNIQUE

Fig. 6 depicts the average throughput versus the user's velocity v for four handover techniques: the NC, the CO technique, the Conv. $\mathcal{V}^{(1)}$ and the Conv. $\mathcal{V}^{(2)}$. It is clear from the figure that at the low velocities regime, where the handover cost is lower, the best performance is achieved by the Conv. $\mathcal{V}^{(2)}$ which provides the highest spectral efficiency. However, it is also the one which has the highest handover rate and therefore it decays to zero throughput the fastest. On the other hand, the CO technique for velocities higher than $v > v^*$ performs better due to the reduced handover rate that is achieved. In addition, the CO technique always outperforms Conv. $\mathcal{V}^{(1)}$, since the CO technique achieves lower handover rate and higher spectral efficiency as a result of the BS cooperation. Furthermore, by comparing the CO with the NC technique, we can see that CO performs better for velocities $v < u^*$. It is worth mentioning, that at u^* the NC technique converges to the alternating skipping technique ($K = 1$). As a result, even though the CO technique offers higher spectral efficiency, the handover cost becomes more critical for very high velocities and so it is more beneficiary for the user to employ the technique which achieves the highest handover rate reduction.

VI. CONCLUSION

This paper proposed two intelligent handover skipping techniques, which allow the user to dynamically skip upcoming handover executions by considering topological characteristics of the network deployment. Firstly, the NC skipping technique considers single BS association and skips a handover based on three criteria: (a) the area of the cell, (b) the trajectory distance within the cell, and (c) the distance of the BS from the cell edge. Our results show that for moderate user's velocities the NC technique offers the highest average throughput. Secondly, the CO skipping technique refers to a user enjoying BS cooperation benefits unless a handover is skipped. The handover decision is taken based on three consecutive cells of the user's trajectory pattern. In contrast to the NC skipping technique, the CO technique limits the randomness of the associated BS during the skipping phase by exploiting topological properties of the second order Voronoi tessellation. It was shown that for moderated and high velocities the CO offers the highest throughput.

APPENDIX

A. HANDOVER SKIP PROBABILITY

A handover skip occurs with probability $\Pi_X(\theta_X) = \mathbb{P}(X \leq \theta_X)$. This is evaluated by using the PDF $f_X(x)$ of the random variable $X \in \{S, L, H\}$ as

$$\Pi_X(\theta_X) = \int_0^{\theta_X} f_X(x)dx, \; X \geq 0. \tag{32}$$

The PDF of the area of the cell S is given by [20]

$$f_S(s) = \frac{3.5^{3.5}}{\Gamma(3.5)} s^{2.5} \exp(-3.5s), \tag{33}$$

where $f_S(s)$ is normalized by $1/\lambda$.

The PDF of the cell chord L is given by [10]

$$f_L(l) = \pi\lambda^{3/2} \int_0^{\pi} \int_0^{\pi-\omega} \frac{\rho_\omega \rho_\phi (2\lambda l^2 \beta^2 \rho_\omega^2 - \gamma) l^2}{\sin(\omega+\phi)\exp(\pi\lambda l^2 V)} d\phi d\omega, \tag{34}$$

where $\beta = (\pi - \phi)\cos\phi + \sin\phi$, $\gamma = (\pi - \phi)\sin\phi\cos\phi$, $V = \left(1 + \rho_\phi^2 - 2\rho_\phi \cos\omega\right)\left(1 - \frac{\phi}{\pi} + \frac{\sin 2\phi}{2\pi}\right) + \rho_\phi^2 \left(1 - \frac{\omega}{\pi} + \frac{\sin 2\omega}{2\pi}\right)$, $\rho_\omega = \frac{\sin\omega}{\sin(\omega+\phi)}$ and $\rho_\phi = \frac{\sin\phi}{\sin(\omega+\phi)}$.

Finally, the PDF of the distance between a BS and the cell edge is given by [21]

$$f_H(h) = \frac{4}{3}\pi\lambda^2 \left(\frac{2h^2}{\sqrt{\lambda}} \exp\left(-\lambda\pi h^2\right) + \operatorname{erfc}\left(h\sqrt{\lambda\pi}\right) \right). \tag{35}$$

B. PROOF OF LEMMA 1

The Laplace transform of the interference term I_n evaluated at s can be derived as

$$\begin{aligned} \mathcal{L}_{I_n}(s) &= \mathbb{E}_\Phi \left[\mathbb{E}_{h_j} \left[\exp\left(-s \sum_{x_j \in \Phi \setminus \mathcal{N}} h_j r_j^{-\alpha} \right) \right] \right] \\ &= \mathbb{E}_\Phi \left[\prod_{x_j \in \Phi \setminus \mathcal{N}} \frac{1}{1 + s r_j^{-\alpha}} \right] \qquad (36) \\ &= \exp\left(-2\pi\lambda \int_{r_n}^{\infty} \left(1 - \frac{1}{1 + s u^{-\alpha}} \right) u du \right), \qquad (37) \end{aligned}$$

where (36) follows from the moment generating function of an exponential random variable and the fact that the variables

h_j are independent and identically distributed; (37) is obtained using the probability generating functional of a PPP [22]. The lower limit r_n ensures that the closest interference is outside the ball centred at the user with radius r_n. After some algebraic manipulations and using [16, 3.194.5], the result follows.

ACKNOWLEDGEMENTS

This paper was presented in part at the IEEE Global Communications Conference 2017, Singapore [1].

REFERENCES

[1] E. Demarchou, C. Psomas, and I. Krikidis, "Intelligent user-centric handover scheme in ultra-dense cellular networks," in *Proc. IEEE Global Commun. Conf.*, Singapore, Dec. 2017, pp. 1–6.
[2] Cisco, "Cisco visual networking index: Global mobile data traffic forecast update, 2016–2021," Cisco, San Jose, CA, USA, White Paper 1454457600805266, Feb. 2017. [Online]. Available: https://www.cisco.com/c/en/us/solutions/collateral/service-provider/visual-networking-index-vni/mobile-white-paper-c11-520862.html
[3] J. G. Andrews *et al.*, "What will 5G be?" *IEEE J. Sel. Areas Commun.*, vol. 32, no. 6, pp. 1065–1082, Jun. 2014.
[4] M. Kamel, W. Hamouda, and A. Youssef, "Ultra-dense networks: A survey," *IEEE Commun. Surveys Tuts.*, vol. 18, no. 4, pp. 2522–2545, 4th Quart., 2016.
[5] S. F. Yunas, M. Valkama, and J. Niemelä, "Spectral and energy efficiency of ultra-dense networks under different deployment strategies," *IEEE Commun. Mag.*, vol. 53, no. 1, pp. 90–100, Jan. 2015.
[6] G. P. Pollini, "Trends in handover design," *IEEE Commun. Mag.*, vol. 34, no. 3, pp. 82–90, Mar. 1996.
[7] A. Racz, A. Temesvary, and N. Reider, "Handover performance in 3GPP long term evolution (LTE) systems," in *Proc. 16th IST Mobile Wireless Commun. Summit*, Budapest, Hungary, Jul. 2007, pp. 1–5.
[8] J. Wu and P. Fan, "A survey on high mobility wireless communications: Challenges, opportunities and solutions," *IEEE Access*, vol. 4, pp. 450–476, 2016.
[9] Y. Hong, X. Xu, M. Tao, J. Li, and T. Svensson, "Cross-tier handover analyses in small cell networks: A stochastic geometry approach," in *Proc. IEEE Int. Conf. Commun.*, London, U.K., Jun. 2015, pp. 3429–3434.
[10] A. Merwaday, I. Güvenç, W. Saad, A. Mehbodniya, and F. Adachi, "Sojourn time-based velocity estimation in small cell poisson networks," *IEEE Commun. Lett.*, vol. 20, no. 2, pp. 340–343, Feb. 2016.
[11] W. Bao and B. Liang, "Stochastic geometric analysis of handoffs in user-centric cooperative wireless networks," in *Proc. IEEE Int. Conf. Comput. Commun.*, San Francisco, CA, USA, Apr. 2016, pp. 1–9.
[12] B. Fang and W. Zhou, "Handover reduction via joint bandwidth allocation and CAC in randomly distributed HCNs," *IEEE Commun. Lett.*, vol. 19, no. 7, pp. 1209–1212, Jul. 2015.
[13] R. Arshad, H. ElSawy, S. Sorour, T. Y. Al-Naffouri, and M.-S. Alouini, "Handover management in dense cellular networks: A stochastic geometry approach," in *Proc. IEEE Int. Conf. Commun.*, Kuala Lumpur, Malaysia, May 2016, pp. 1–7.
[14] R. Arshad, H. ElSawy, S. Sorour, T. Y. Al-Naffouri, and M.-S. Alouini, "Cooperative handover management in dense cellular networks," in *Proc. IEEE Global Commun. Conf.*, Washington, DC, USA, Dec. 2016, pp. 1–6.
[15] R. Arshad, H. Elsawy, S. Sorour, T. Y. Al-Naffouri, and M.-S. Alouini, "Handover management in 5G and beyond: A topology aware skipping approach," *IEEE Access*, vol. 4, pp. 9073–9081, 2016.
[16] I. S. Gradshteyn and I. M. Ryzhik, *Table of Integrals, Series, and Products*. New York, NY, USA: Elsevier, 2007.
[17] D. Moltchanov, "Distance distributions in random networks," *Ad Hoc Netw.*, vol. 10, no. 6, pp. 1146–1166, 2012.
[18] X. Ge, J. Ye, Y. Yang, and Q. Li, "User mobility evaluation for 5G small cell networks based on individual mobility model," *IEEE J. Sel. Areas Commun.*, vol. 34, no. 3, pp. 528–541, Mar. 2016.
[19] C. Hoymann, D. Larsson, H. Koorapaty, and J.-F. Cheng, "A lean carrier for LTE," *IEEE Commun. Mag.*, vol. 51, no. 2, pp. 74–80, Feb. 2013.
[20] J.-S. Ferenc and Z. Néda, "On the size distribution of Poisson Voronoi cells," *Phys. A, Statist. Mech. Appl.*, vol. 385, no. 2, pp. 518–526, Nov. 2007.
[21] L. Muche, "The Poisson–Voronoi tessellation: Relationships for edges," *Adv. Appl. Probab.*, vol. 37, pp. 279–296, Jun. 2005.
[22] M. Haenggi, *Stochastic Geometry for Wireless Networks*. Cambridge, U.K.: Cambridge Univ. Press, 2013.

ELENI DEMARCHOU (S'16) received the B.Sc. degree in electrical engineering from the University of Cyprus, Cyprus, in 2014, and the M.Sc. degree in wireless communications from The University of Southampton, U.K., in 2015. She is currently pursuing the Ph.D. degree in electrical engineering with the University of Cyprus. She joined the KIOS Research and Innovation Center of Excellence, University of Cyprus, as a Researcher, in 2015. Her research interests focus on wireless communications.

CONSTANTINOS PSOMAS (M'15) received the B.Sc. degree in computer science and mathematics from Royal Holloway, University of London, U.K., in 2007, the M.Sc. degree in applicable mathematics from the London School of Economics, U.K., in 2008, and the Ph.D. degree in mathematics from The Open University, U.K., in 2011. From 2011 to 2014, he was a Post-Doctoral Research Fellow with the Department of Electrical Engineering, Computer Engineering and Informatics, Cyprus University of Technology. He is currently a Post-Doctoral Researcher with the KIOS Research and Innovation Center of Excellence, University of Cyprus. His current research interests include full-duplex radio, wireless powered communications, and cooperative networks.

IOANNIS KRIKIDIS (S'03–M'07–SM'12) received the Diploma degree in computer engineering from the Computer Engineering and Informatics Department, University of Patras, Greece, in 2000, and the M.Sc. and Ph.D. degrees in electrical engineering from the Ecole Nationale Superieure des Telecommunications (ENST), Paris, France, in 2001 and 2005, respectively. From 2006 to 2007, he was a Post-Doctoral Researcher with ENST, and from 2007 to 2010, he was a Research Fellow with the School of Engineering and Electronics, The University of Edinburgh, Edinburgh, U.K. He has also held research positions with the Department of Electrical Engineering, University of Notre Dame; with the Department of Electrical and Computer Engineering, University of Maryland; with the Interdisciplinary Centre for Security, Reliability and Trust, University of Luxembourg; and also with the Department of Electrical and Electronic Engineering, Niigata University, Japan. He is currently an Assistant Professor with the Department of Electrical and Computer Engineering, University of Cyprus, Nicosia, Cyprus. His current research interests include communication theory, wireless communications, cooperative networks, cognitive radio, and wireless powered communications. Dr. Krikidis received the Research Award-Young Researcher from the Research Promotion Foundation, Cyprus, in 2013, and the IEEE ComSoc Best Young Professional Award in Academia in 2016. He serves as an Associate Editor for the IEEE Transactions on Communications, the IEEE Transactions on Green Communications and Networking, and the IEEE Wireless Communications Letters. He was the Technical Program Co-Chair of the IEEE International Symposium on Signal Processing and Information Technology 2013 and the Lead Guest Editor of the Special Issue on Exploiting Interference towards Energy Efficient and Secure Wireless Communications, the IEEE Journal of Selected Topics in Signal Processing, 2016.